Utilization of Fluoroethene as a Surrogate for Aerobic Vinyl Chloride Transformation

ANNE E. TAYLOR,[†] MARK E. DOLAN,[†]
PETER J. BOTTOMLEY,[‡] AND
LEWIS SEMPRINI*,[†]

School of Chemical, Biological and Environmental Engineering, 101 Gleeson Hall, and Department of Microbiology, 220 Nash Hall, Oregon State University, Corvallis, Oregon 97331

Fluoroethene (FE) is a stable molecule in aqueous solution and its aerobic transformation potentially yields F^-. This work evaluated if FE is a suitable surrogate for monitoring aerobic vinyl chloride (VC) utilization or cometabolic transformation. Experiments were carried out with three isolates, *Mycobacterium* strain EE13a, *Mycobacterium* strain JS60, and *Nocardioides* strain JS614 to evaluate if their affinities for FE and VC and their rates of transformation were comparable and whether the transformation of FE and F^- accumulation could be correlated with VC utilization. JS614 grew on FE in addition to VC, making it the first organism reported to use FE as a sole carbon and energy source. EE13a cometabolized VC and FE, and JS60 catabolized VC and cometabolized FE. There was little difference among the three strains in the K_s or k_{max} values for VC or FE. Competitive inhibition modeled the temporal responses of FE and VC transformations and Cl^- and F^- release when both substrates were present. Both the rate of FE transformation and rate of F^- accumulation could be correlated with the rate of aerobic transformation of VC and showed promise for estimating VC rates in situ using FE as a reactive surrogate.

Introduction

Anaerobic reductive dechlorination can reduce the industrial solvents perchloroethene (PCE) and trichloroethene (TCE) completely to ethene (Eth) when site conditions and electron donor availability are ideal, but the daughter products *cis*-dichloroethene (cDCE) and vinyl chloride (VC) can accumulate if conditions are not favorable (*1*). VC is more water-soluble and has a lower octanol/water partitioning coefficient (K_{ow}) than either PCE or TCE and sorbs less strongly to aquifer materials (*2*). As a result, VC can be transported out of the anaerobic zone where reductive processes are occurring and into zones where soluble oxygen is present, potentially allowing aerobic processes to occur. Organisms possessing oxygenases with broad substrate specificity including butane, methane, propane, and ammonia monooxygenase are capable of cometabolically transforming VC by oxidizing its double bond (*3*). The resulting epoxide, chlorooxirane, is unstable and spontaneously degrades, yielding a mixture of acetylchloride, glycoaldehyde, chloroacetaldehyde, and chloride (Cl^-) (*4*, *5*). Also widely distributed in the environment are bacteria that can utilize VC as a sole carbon and energy source (*6*). VC-assimilating bacteria from the genera *Mycobacterium, Nocardioides, Ochrobactrum, Pseudomonas,* and *Ralstonia* have been isolated from contaminated and non-contaminated sites (*6*, *7*). Although phenotypically diverse, the bacteria that mineralize VC all utilize Eth as a growth substrate, and oxidation of Eth and VC is initiated by an alkene monooxygenase (AkMO) (*6*–*11*).

It is difficult to estimate rates of aerobic VC transformation in situ because the mineralization of VC yields CO_2 and Cl^-, neither of which can be tied solely to VC transformation. Stable carbon isotope fractionation can distinguish between biodegraded and abiologically degraded VC and can determine whether biodegradation of VC was aerobic or anaerobic, but it has not been utilized to estimate rates of VC degradation (*12*, *13*). Utilizing a surrogate for VC that is transformed via the same enzyme systems, but would yield a discrete analytical response when aerobically metabolized would allow estimation of VC transformation rates in contaminated aquifers.

In reductive dechlorination systems, trichlorofluoroethene (TCFE) has been used as a surrogate for TCE transformation in situ and in microcosm tests, and 1-chloro-1-fluoroethene (1,1-CFE) and *E*-chlorofluoroethene (E-CFE) have served as analogues for VC in microcosm and field push–pull tests (*14*–*16*). In these reductive systems using a fluorinated surrogate, the accumulation of fluoroethene (FE) was correlated with the formation of ethene from VC (*15*). FE is a stable molecule in aqueous solution and its aerobic degradation yields fluoride (F^-), which is a unique signature in most aquifers. Work with cytochrome P450-dependent monooxygenases suggests that FE is aerobically degraded in a manner similar to VC; an epoxide is formed from the initial oxidation (*17*, *18*). FE-epoxide is unstable and is expected to yield spontaneous degradation products analogous to VC-epoxide (*4*, *5*). To our knowledge, no bacterium has been reported to oxidize or utilize FE as a sole carbon and energy source, although the similarity of its structure to VC would suggest that the oxidation of the double bond is possible.

The objective of this work was to evaluate if FE is a suitable surrogate for monitoring aerobic VC utilization or cometabolic transformation. Laboratory experiments were carried out with various oxygenase-containing aerobic bacteria that either cometabolically or catabolically metabolize VC, to evaluate if (i) rates of FE transformation are similar to those of VC transformation, (ii) VC and FE have similar affinities for the monooxygenase that mediates the initial transformation, (iii) a competitive inhibition kinetic model accurately simulates concurrent FE and VC degradation, and (iv) the rate of F^- accumulation can be correlated with that of VC utilization. In addition, the potential for bacteria to use FE as a carbon and energy source was evaluated.

Materials and Methods

Chemicals and Medium. VC (99.5%), TCE (99.9%), acetylene, and propyne (97%) were obtained from Aldrich (Milwaukee, WI), FE (98%) from SynQuest (Alachua, FL), and Eth (C.P. grade) from Airgas (Radnor, PA). Cells were grown in a minimal salts medium (MSM) (*6*). One-tenth-strength tryptic soy agar (TSA) was used as a nonselective media and contained 3 g of Bacto tryptic soy powder (Difco), 10 g of glucose, and 15 g of agar/L.

* Corresponding author phone: 541-737-6895; fax: 541-737-3052; e-mail: lewis.semprini@orst.edu.
† Department of Civil, Construction and Environmental Engineering.
‡ Department of Microbiology.

Cultures and Maintenance. Strain EE13A was isolated from chloroethene-contaminated groundwater collected from well LC191, Ft. Lewis, WA. The groundwater was contaminated with both cDCE and TCE and contained dissolved oxygen (*19*). Isolation was achieved by streaking an Eth enrichment culture incubated at room temperature (23 °C) on TSA plates and subculturing individual colonies on MSM with Eth provided as the sole carbon source. Repeated streaking and culturing eventually yielded a strain that utilizes Eth as a growth substrate and cometabolically degrades VC and FE. Identification of strain EE13a was done by partial sequencing of amplified 16S rDNA at the Center for Genome Research and Biocomputing at Oregon State University on an ABI Prism 3730 Genetic Analyzer, Applied Biosystems (Foster City, CA), and the 16S rDNA gene sequence was deposited in GenBank under the accession number EF405863. The partial 16S rDNA of strain EE13a (900 bp) shared 99% sequence identity with *Mycobacterium* sp. O228YA isolated from a dioxin-contaminated landfill in Japan (*20*) and 96% similarity with *Mycobacterium* strain JS60. *Mycobacterium* strain JS60 and *Nocardioides* sp. strain JS614 utilize Eth and VC as sole carbon and energy sources (*6*) and were provided by Dr. Jim Spain (Georgia Tech University, Atlanta, GA). All cultures were grown in 500 mL glass Wheaton bottles sealed with phenolic caps and gray butyl rubber septa, in 200 mL of MSM and either 4% (v/v) headspace Eth, FE, or VC added as the sole carbon and energy source. Cultures were shaken inverted, at 120 rpm in a Brunswick controlled environment shaker at 29 ± 1 °C. Growth was followed by monitoring the increase in optical density (OD) at 600 nm. For experimental use, cells were harvested at mid-log phase by centrifugation. Cells were pelleted and washed twice in 4 mM potassium phosphate buffer at pH 7.0. Cell pellets were held at room temperature (<15 min) and resuspended to a dense concentration (40−60 mg of protein/mL) in phosphate buffer immediately before initiating an experiment.

Analytical Methods. A microbiuret assay was used to determine the protein content of cells in the batch reactors used in kinetic tests (*21*). Progress curves of Eth, VC, and FE disappearance were constructed by analyzing headspace samples (100 or 500 μL) by gas chromatography (GC) with flame-ionization detection (FID) using a Shimadzu (Kyoto, Japan) GC-14A gas chromatograph fitted with an Alltech (Deerfield, IL) AT-1 capillary column (0.53 mm × 15 m). The FID and injector temperatures were adjusted to 200 °C and the column temperature was adjusted to 70 °C. The mass of substrate remaining during kinetic tests was calculated from the concentration in the headspace samples using Henry's Law.

Concentrations of Cl$^-$ and F$^-$ were determined using ion chromatography analysis. Aqueous samples were withdrawn through the gray butyl septa during the short-term kinetic studies, filtered through 0.45 μm pore size cellulose acetate membrane filters into 2 mL of auto sampler vials sealed with crimp caps, and amended with 5% propyne. Samples were incubated with propyne for 1 h to inhibit any residual activity by cells that may have passed through the membrane filter and were then transferred to microcentrifuge tubes and stored at 4 °C until analysis. Cl$^-$ and F$^-$ concentrations were determined using a Dionex DX-500 Ion Chromatograph (Sunnyvale, CA) equipped with an electrical conductivity detector and a Dionex AS14 column.

Determination of Kinetic Parameters. Kinetic parameters were obtained from batch kinetic tests using resting cells grown and harvested as described above. VC and FE disappearance and halide release batch tests were carried out in 155 mL serum bottles sealed with phenolic caps and gray butyl rubber septa and contained 100 mL of 4 mM phosphate buffer, pH 7.0. Specific amounts of gases were added to achieve desired aqueous concentrations based on Henry's Law and were incubated with shaking at 150 rpm at room temperature, 23 ± 2 °C, to achieve phase equilibrium. Experiments were initiated by adding aliquots of a dense cell suspension (typically 100 μL) to the bottles. The initial concentrations of substrates were significantly greater than K_s or K_c values (half-velocity coefficients for growth and nongrowth substrates, respectively, μM) and transformation was followed to completion. Eth, FE, or VC utilization or transformation progress curves were fitted using a weighted nonlinear least-squares analysis of the integrated Monod equation to estimate the kinetic parameters k_{max} (maximum specific substrate utilization rate, nmol/min/mg of protein) and $K_{s/c}$ (*22*). All experiments were carried out in triplicate and k_{max} and $K_{s/c}$ were estimated from each progress curve and then averaged. The generation time was determined by monitoring the optical density at 600 nm. Dry weight was determined by filtering a volume of cell culture on a 0.2 μm membrane, then dried at 65 °C, and weighed. This dry weight was correlated with cell culture optical density at 600 nm for the yield determination. Transformation capacity (T_c) values for the nongrowth substrates were determined by incubating Eth-grown cultures with nongrowth substrates and transformation was monitored until it ceased. Abiotic controls showed minimal losses of substrate over the time course of the experiments (<120 min).

The possibility of mass-transfer limitations between the aqueous and gas phases was evaluated by inoculating bottles prepared as previously described with 1X and 2X cell concentration and comparing the rates of substrate transformation. Rates of degradation in the bottles with 2X cells were twice the rates of the bottles with 1X cells (data not shown), indicating mass transfer did not limit the rate of biological reactions under the experimental conditions. To eliminate concerns that oxygen limited rates of transformation, a second aliquot of gas substrate was added to the batch tests after the completion of a progress curve and transformation followed. Rates of transformation for the second progress curve were similar to those of the first (data not shown), indicating that oxygen did not limit rates.

Modeling Experimental Data. The kinetic parameters from the nonlinear least-squares analysis were used to model progress curves in the presence of two substrates to identify the inhibition type. The model incorporated partitioning between gas and liquid compartments (55 and 100 mL, respectively) using dimensionless Henry's coefficients of 7.24 for Eth, 0.99 for VC, and 2.66 for FE determined at room temperature (23 ± 2 °C) (*7*, *15*, *23*), and the assumption was made that halide release occurred instantaneously with transformation. Stoichiometry of halide release was determined and incorporated into the model. The non-steady-state, nonlinear equations were solved simultaneously using STELLA 8.1.1 (isee systems, Lebanon, NH). The assumption was made that cell concentration did not change due to cell growth over the course of the short experiments (<120 min) because these bacteria are slow growing (generation time >24 h at 23 °C, data not shown) and that cell death did not occur since the amounts of nongrowth substrates transformed were well below T_c. Competitive, noncompetitive, and uncompetitive inhibition models were used to model experimental data (*24*) (Supporting Information, eqs S1−6). The independently determined kinetic parameters, k_{max} and $K_{s/c}$, and initial concentration of substrate were held constant while solving two equations simultaneously for VC as substrate and FE as an inhibitor, and vice versa. The inhibition constant K_i was adjusted to refine the fit of the model to the experimental data. The experimental data were plotted against the model output and r^2 was calculated by linear least-squares regression to determine the goodness of fit. The sum of squares error (SSE) between the experimental

isolate	sub-strate	generation time (h)	Y (g of protein/mol of substrate)	Y (g of bio-mass COD/g of substrate COD)	T_c (μmol/mg dry weight)
EE13a	Eth	18.3 (2.9)	7.4 (0.5)	0.22	
	VC	no growth			43.3 (1.5)
	FE	no growth			40.7 (2.0)
JS60	Eth	15.6 (0.5)	9.1 (1.3)	0.27	
	VC	27.4 (0.5)	4.3 (0.3)	0.14	
	FE	no growth			36.6 (3.0)
JS614	Eth	17.8 (2.3)	10.3 (1.8)	0.30	
	VC	17.5 (0.9)	7.3 (0.2)	0.24	
	FE	18.5 (0.5)	6.2 (0.5)	0.20	

[a] Substrates that did not support growth are indicated by "no growth" and there are no values for generation time or yield. T_c represents cometabolic transformation capacity and there are no values for growth substrates. Standard deviations of three replicates are in parentheses.

isolate	substrate	k_{max} (nmol/min/mg of protein)	$K_{s/c}$ (μM)	K_i (μM)
EE13a	Eth	31.1 (0.8)	1.5 (0.1)	ND
	FE	34.9 (9.4)	1.4 (0.8)	0.5
	VC	30.0 (11.6)	0.8 (0.3)	2.9
JS60	Eth	23.8 (2.8)	1.0 (0.4)	ND
	FE	38.2 (6.6)	1.3 (0.4)	1.0
	VC	36.0 (6.1)	0.9 (0.4)	0.1
JS614	Eth	41.1 (2.6)	1.4 (0.2)	ND
	FE	31.4 (6.8)	1.0 (0.6)	1.5
	VC	29.8 (2.6)	1.4 (0.1)	3.5

[a] The estimates were obtained using a nonlinear least-squares method (22). The standard deviations of three replicates are in parentheses. K_i values gave the best fit for the experimental data in Figure 2. ND = not determined.

data and the model output was also calculated to evaluate how well the model simulated the experimental data.

Results

Early in the research, growth-linked transformation of FE was observed for JS614 (Table 1). The discovery that this bacterium utilized FE for growth and energy provided the opportunity to test our experimental objectives against a suite of bacteria with three distinct phenotypes. While doubling times and growth yields (Y, g of protein/mol of substrate) on Eth were similar for all three strains, the doubling time for JS60 on VC was longer than that for JS614 (27.4 vs 17.5 h), and JS614 had a proportionally greater growth yield during growth on VC. With FE as the sole carbon and energy source, JS614 produced a yield and generation time similar to those for VC. Growth yield for JS60 when VC was the substrate was 47% of the yield when Eth was the growth substrate. Decreases in yield for JS614 on the halogenated ethenes in comparison with Eth were less dramatic than those for JS60, and the doubling times on VC and FE were very similar to those for Eth. Yields expressed in terms of COD illustrate that JS614 is more efficient than JS60 at incorporating VC-carbon into biomass, or better able to overcome toxic effects of VC-epoxide. Lower yields for JS60 and JS614 than those reported by Coleman et al. (6) are possibly due to the indirect method Coleman employed to estimate protein yield. The T_c of VC and FE during cometabolic transformation by EE13a were similar and were comparable to the T_c of JS60 when FE was transformed (Table 1).

Despite the fact that the three VC-degrading isolates responded differently to Eth, VC, and FE as growth substrates, there were little difference between the $K_{s/c}$ or k_{max} values for FE and VC of any individual isolate, and there was little difference between the three isolates in their rates of transformation or affinity for the halogenated substrates (Table 2). Additionally, rates of maximum VC and FE transformation or utilization were similar for all three isolates, indicating that the presence of the smaller F atom did not affect the AkMO's ability to accept FE as a substrate. Values of k_{max} were different than those previously reported for JS614 and JS60 (6), but could be attributed to growth condition differences and the use of Eth-grown cells in this work while VC and Eth-grown cells were used formerly.

Competition experiments were performed to evaluate how FE was transformed in the presence of VC. For these tests the initial aqueous concentration of VC was held constant at a concentration above the K_s (~20 μM), and FE concen-

trations were varied (0, and ~20, 40, 60, and 80 μM). When initial aqueous concentrations of FE and VC were both ~20 μM, the cotransformation rates of FE by EE13a, JS60, and JS614 were 58, 65, and 37% of the rate of the FE-only control, while the rates of cotransformation for VC were 50, 43, and 66% of the VC-only control (Figure 1). As initial aqueous concentrations of FE were increased, and the initial aqueous VC concentration was held constant, inhibition of FE transformation by VC was overcome and rates of FE cotransformation by EE13a and JS60 increased to rates comparable to those achieved when VC was not present, indicating inhibition was competitive for these two organisms (Figure 1A). In contrast, although cotransformation rates of FE by JS614 also increased with FE concentration, the maximum cotransformation rate was only 57% of that achieved when FE was the sole substrate (Figure 1A), and a slightly higher rate of residual VC cotransformation was retained (Figure 1B).

The independently determined $K_{s/c}$ and k_{max} in Table 2 could be utilized to model temporal responses when FE and VC were both present using a competitive inhibition model, but values for K_i were unknown. The initial assumption was made that K_i was equal to the measured $K_{s/c}$ values. This assumption was a good approximation for VC and 1,1-CFE in a reductive system where they inhibited each other (15), but in an aerobic mixed culture of butane-utilizing bacteria the K_i equals K_s assumption was not always valid when modeling concurrent utilization of growth substrate and transformation of nongrowth substrates 1,1,1-trichloroethane, 1,1-dichloroethane, and 1,1-dichloroethene (25).

Competitive inhibition was modeled for the specific case where the initial aqueous concentrations of VC and FE were equal (~20 μM) and X, k_{max}, and $K_{s/c}$ were held constant, and K_i was heuristically varied from the measured $K_{s/c}$ value to provide better fits to the experimental data. (Results are presented in the Supporting Information, Table S1, Figure S1). Making changes in K_i improved the SSE for all three isolates by an order of magnitude. These kinetic parameters also successfully modeled competitive inhibition as the FE concentrations increased (Figure S1). Because the FE cotransformation rates of JS614 showed a lesser response to increases in FE concentration in the presence of VC, experimental data were also modeled with uncompetitive and noncompetitive models. These models produced SSE an order of magnitude greater than the competitive inhibition model, and for the uncompetitive and noncompetitive models to approach a fit equal to the competitive inhibition model, a 10-fold increase in k_{max} was required (data not shown).

In a separate experiment we also determined if it was possible to monitor VC transformation by modeling the rates
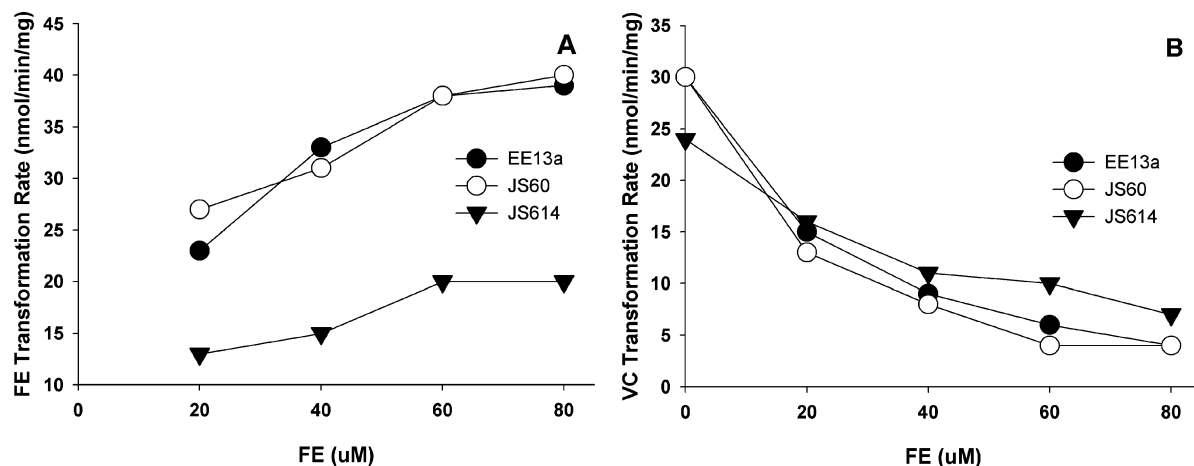
FIGURE 1. Rates of cotransformation by VC-degrading isolates during competition experiments where VC and FE were in the same batch reactor. VC aqueous concentrations were initially at ~20 μM and FE aqueous concentrations initially set at 0 and ~20, 40, 60, and 80 μM. (A) Response of the FE cotransformation rate to increasing FE concentration and fixed VC initial concentration (~20 μM). Maximum rates of FE transformation in the absence of VC were determined at 20 μM and were 40, 41, and 35 nmol/min/mg of protein for EE13a, JS60, and JS614, respectively. (B) Response of the VC cotransformation rate to increasing FE concentration and VC concentration (~20 μM).
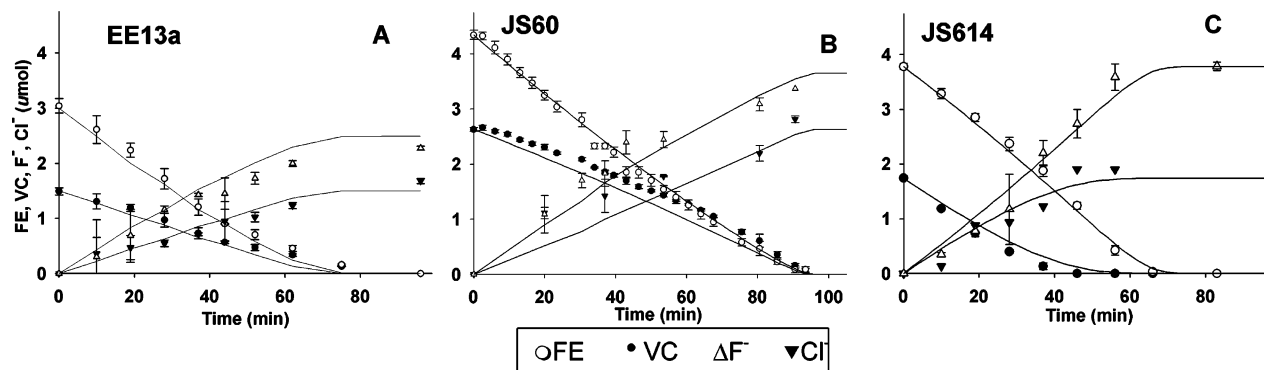

FIGURE 2. VC and FE transformation and Cl⁻ and F⁻ release (symbols) for each of the VC-degrading isolates. Error bars represent the standard deviation of three replicates. The solid lines represent the competitive inhibition modeling of substrate transformation and halide release.

TABLE 3. Rates of Cotransformation of FE and VC and Rates of F⁻ and Cl⁻ Release in Batch Reactors at Equal Starting Aqueous Concentrations of FE and VC (~20 μM)[a]

isolate	substrate	transformation rate (nmol/min/mg of protein)	halide release rate (nmol/min/mg of protein)
EE13a	FE	22.3 (0.1)	18.0 (1.3)
	VC	9.6 (0.3)	8.2 (1.8)
JS60	FE	22.0 (3.3)	19.0 (2.9)
	VC	6.4 (0.7)	6.9 (0.3)
JS614	FE	11.6 (1.5)	13.9 (1.2)
	VC	18.2 (0.2)	20.6 (3.6)

[a] The standard deviations of three replicates are in parentheses.

of F⁻ accumulation. During cotransformation, the initial rates of halide release matched that of substrate transformed for each VC-degrading isolate (Table 3), and in separate experiments where the degradation of individual substrates was followed, halide release ceased as soon as substrate transformation was complete. This demonstrated that there was no further halide release from halogenated products that might have been formed during cometabolism (data not shown). For VC, mass balance of the substrate transformed and halide released was nearly stoichiometric regardless of whether it was a growth or nongrowth substrate and averaged 0.98 (±0.11) on a mole fraction basis. There was a trend for

stoichiometric release of F⁻ during transformation of FE by JS614 (1.0 ± 0.16 mol %), while F⁻ released during cometabolic transformation of FE by EE13a and JS60 averaged 0.84 (±0.04) mol %. Competitive inhibition between substrates, halide release rates equivalent to substrate transformation rates, a known mole fraction of halide released, and previously determined X, k_{max}, and $K_{s/c}$ values were incorporated into the model. This model accurately estimated the accumulation of halide in the batch reactors using heuristically fit K_i values (Table 2, Figure 2). K_i values can deviate between experiments, as they did in our case (26). In the case of EE13a, K_i values for FE and VC, neither of which are growth substrates, were the same in both the competition experiment (Supporting Information, Table S1, Figure S1) and the halide release experiment (Figure 2), but this was not the case for JS60 and JS614, which can utilize one or both VC and FE as growth substrates.

Discussion

To our knowledge, JS614 is the first microorganism reported to grow aerobically on FE. Similar growth yields for JS614 when utilizing FE or VC, along with similar kinetics of utilization, suggest that the same metabolic pathway is utilized for both substrates. It will be interesting to determine what steps in the metabolism of VC by JS60 differ from those in JS614 and thereby prevent growth of the former on FE. The proposed pathway for VC metabolism by JS614 and JS60 show Cl⁻ release as a spontaneous reaction (27, 28), but it

is unknown if F^- release would utilize the same mechanism as Cl^- release. Differences between JS614 and JS60 have previously been noted; Y is much greater for JS614 than for JS60 when VC is the sole carbon and energy source (6) (Table 1). That observation, plus new observations from this work, (i) the ability of JS614 to grow on FE with a yield similar to that for VC and (ii) different response to competing substrates (Figure 1), indicate that JS614's VC metabolic pathway may differ from JS60's.

For the three aerobic VC-degrading isolates studied, both the rates of FE transformation and F^- accumulation could be correlated with the rate of aerobic degradation of VC. FE therefore has the potential to be used as a surrogate reactive tracer for estimating rates of VC degradation in situ. In a VC-contaminated aquifer, for example, in single-well push–pull tests, FE addition and subsequent cotransformation could be utilized as an indicator of in situ VC transformation rates. Although fluorinated surrogates must be considered as their chlorinated analogues (29), they have been previously utilized in situ in reductive dechlorinating systems to estimate rates of VC transformation with the expectation that FE would accumulate (14, 16). In single-well push–pull tests, rates of transformation of the analogue for VC under dechlorinating conditions, E-CFE, have been used to estimate rates of VC transformation (16). Because the reduction of E-CFE results in FE, its formation and subsequent transformation and accumulation of F^- could be exploited to determine if sequential anaerobic/aerobic processes are transforming TCE and its daughter products to nontoxic end products. As far as is known, FE is not transformed in anaerobic systems (15) and the accumulation of F^- would be a potential indicator that VC is being degraded aerobically.

During injection for a push–pull test, a solution with a low concentration of FE would mix with native groundwater and VC and FE may both be present. This would require that competitive inhibition of the two substrates be taken into consideration when estimating rates of VC transformation. The average inhibition of rates of FE transformation at equal VC and FE concentrations was 53 (±14)% (Figure 1). When this average is applied to the F^- release data in Table 3, estimates of VC transformation rates are 113, 99, and 88% of k_{max} values reported in Table 2 for EE13a, JS60, and JS614, respectively. Furthermore, there is the potential for the detection of very low rates of F^- release. The ion chromatographic method used in this work had a detection limit of approximately 7 μM, but detection of F^- with an ion-selective electrode has been reported in the range of 0.01 μM (30).

FE was transformed by VC-degrading bacteria with a significant and measurable release of halide. F^- release during aerobic transformation has been reported from fluorophenols by an activated sludge, fluorosulfonates by *Pseudomonas* sp. strain D2, and fluorinated anilines by *Pseudomonas fluorescens* 26-K (30–32). F^- release has also been observed during the aerobic cometabolism of a variety of chlorofluorocarbons by the methanotroph *Methylosinus trichosporium* OB3b and the propane utilizing *Mycobacterium vaccae* JOB5 (33). Ours is the first report of release of F^- release during aerobic FE transformation by VC-degrading bacteria. The release of F^- during the cometabolic transformation of FE by EE13a and JS60 implies that an unstable epoxide was formed during the initial transformation by a bacterial monooxygenase and is consistent with the observations made during transformation by cytochrome P450-dependent monooxygenases (17, 18).

Aerobic VC-degrading bacteria like those in this study with high affinity for VC ($K_{s/c} \sim 1\,\mu$M) and high transformation capacities can be important in the remediation of VC-contaminated aquifers. Ethene formed during the slow cometabolic reductive dechlorination of VC could support VC-utilizing bacteria in the aerobic fringe of the anaerobic zone. The complimenting limitations and capabilities of anaerobic (higher affinity for TCE and cDCE) and aerobic (higher affinity for VC) microorganisms illustrate the importance of understanding both processes in the detoxification of chlorinated solvent contamination.

Acknowledgments

Supporting Information Available

Equations, additional table and figure. This material is available free of charge via the Internet at http://pubs.acs.org.

Literature Cited

(1) Christ, J. A.; Ramsburg, C. A.; Abriola, L. M.; Pennell, K. D.; Loffler, F. E. Coupling aggressive mass removal with microbial reductive dechlorination for remediation of DNAPL source zones: a review and assessment. *Environ. Health Perspect.* **2005**, *113*, 465−477.

(2) Schnoor, J. L. *Environmental modeling. Fate and transport of pollutants in water, air, and soil*; Wiley-Interscience: New York, 1996.

(3) Arp, D. J.; Yeager, C. M.; Hyman, M. R. Molecular and cellular fundamentals of aerobic cometabolism of trichloroethylene. *Biodegradation* **2001**, *12*, 81−103.

(4) Bolt, H. M. Roles of etheno-DNA adducts in tumorigenicity of olefins. *Crit. Rev. Toxicol.* **1988**, *18*, 299−309.

(5) Ballering, L. A.; Nivard, M. J.; Vogel, E. W. Characterization by two-endpoint comparisons of the genetic toxicity profiles of vinyl chloride and related etheno-adduct forming carcinogens in Drosophila. *Carcinogens* **1996**, *17*, 1083−1092.

(6) Coleman, N. V.; Mattes, T. E.; Gossett, J. M.; Spain, J. C. Phylogenetic and kinetic diversity of aerobic vinyl chloride-assimilating bacteria from contaminated sites. *Appl. Environ. Microbiol.* **2002**, *68*, 6162−6171.

(7) Elango, V. K.; Liggenstoffer, A. S.; Fathepure, B. Z. Biodegradation of vinyl chloride and *cis*-dichloroethene by *Ralstonia* sp. strain TRW-1. *Appl. Microbiol. Biotechnol.* **2006**, *72*, 1270−1275.

(8) Hartemans, S.; deBont, J. A. M. Aerobic vinyl chloride metabolism in *Mycobacterium aurum* L1. *Appl. Environ. Microbiol.* **1992**, *58*, 1220−1226.

(9) Danko, A. S.; Luo, M. Z.; Bagwell, C. E.; Brigmon, R. L.; Freedman, D. L. Involvement of linear plasmids in aerobic biodegradation of vinyl chloride. *Appl. Environ. Microbiol.* **2004**, *70*, 6092−6097.

(10) Fathepure, B. Z.; Elango, V. K.; Singh, H.; Bruner, M. A. Bioaugmentation potential of a vinyl chloride-assimilating *Mycobacterium* sp., isolated from a chloroethene-contaminated aquifer. *FEMS* **2005**, *248*, 227−234.

(11) Verce, M. F.; Freedman, D. L. Modeling the kinetics of vinyl chloride cometabolism by an ethane-grown *Pseudomonas* sp. *Biotechnol. Bioeng.* **2001**, *71*, 274−285.

(12) Chartrand, M. M. G.; Waller, A.; Mattes, T. E.; Elsner, M.; Lacrampe-Couloume, G.; Edwards, E. A.; Lollar, B. S. Carbon isotopic fractionation during aerobic vinyl chloride degradation. *Environ. Sci. Technol.* **2005**, *39*, 1064−1070.

(13) Chu, K. H.; Mahendra, S.; Song, D. L.; Conrad, M. E.; Alvarez-Cohen, L. Stable carbon isotope fractionation during aerobic biodegradation of chlorinated ethenes. *Environ. Sci. Technol.* **2004**, *38*, 3126−3130.

(14) Hageman, K. J.; Istok, J.; Field, J.; Buscheck, T. E.; Semprini, L. In situ anaerobic transformation of trichlorofluoroethene in trichloroethene-contaminated groundwater. *Environ. Sci. Technol.* **2001**, *35*, 1729−1735.

(15) Pon, G.; Semprini, L. Anaerobic reductive dechlorination of 1-chloro-1-fluoroethene to track the transformation of vinyl chloride. *Environ. Sci. Technol.* **2004**, *38*, 6803−6808.

(16) Ennis, E.; Reed, R.; Dolan, M.; Semprini, L.; Istok, J.; Field, J. Reductive dechlorination of the vinyl chloride surrogate chlorofluoroethene in TCE-contaminated groundwater. *Environ. Sci. Technol.* **2005**, *39*, 6777−6785.

(17) Csandy, G. A.; Laib, R. J.; Filser, J. G. Metabolic transformation of halogenated and other alkenes—a theoretical approach. Estimation of metabolic reactivities for in vivo conditions. *Toxicol. Lett.* **1995**, *75*, 217−223.

(18) Cantoreggi, S.; Keller, D. A. Pharmacokinetics and metabolism of vinyl fluoride in vivo and in vitro. *Toxicol. Appl. Pharmacol.* **1997**, *143*, 130−139.

(19) Azizian, M. F.; Istok, J. D.; Semprini, L. Evaluation of the *in-situ* aerobic cometabolism of chlorinated ethenes by toluene-utilizing microorganisms using push-pull tests. *J. Contam. Hydrol.* **2007**, *90*, 105−124.

(20) Wang, Y.; Ogawa, M.; Fukuda, K.; Miyamoto, H.; Taniguchi, H. Isolation and identification of Mycobacteria from soils at an illegal dumping site and landfills in Japan. *Microbiol. Immunol.* **2006**, *50*, 513−524.

(21) Gornall, A. G.; Bardawill, C. J.; David, M. M. Determination of serum proteins by means of the biuret reaction. *J. Biol. Chem.* **1949**, *177*, 751−766.

(22) Smith, L. H.; McCarty, P. L.; Kitanidis, P. Spreadsheet method for evaluation of biochemical reaction rate coefficients and their uncertainties by weighted nonlinear least-squares analysis of the integrated Monod equation. *Appl. Environ. Microbiol.* **1998**, *64*, 2044−2050.

(23) Gossett, J. M. Measurement of Henry's law constants for C_1 and C_2 chlorinated hydrocarbons. *Environ. Sci. Technol.* **1987**, *58*, 202−208.

(24) Morris, J. G. *A Biologist's Physical Chemistry*; William Clowes and Sons, Limited: London, 1970.

(25) Kim, Y.; Arp, D. J.; Semprini, L. Kinetic and inhibition studies for the aerobic cometabolism of 1,1,1-trichloroethane, 1,1-dichloroethylene, and 1,1-dichloroethane by a butane-grown mixed culture. *Biotechnol. Bioeng.* **2002**, *80*, 498−508.

(26) Kim, Y.; Arp, D. J.; Semprini, L. A combined method for determining inhibition type, kinetic parameters, and inhibition coefficients for aerobic cometabolism of 1,1,1-trichloroethane by a butane-grown mixed culture. *Biotechnol. Bioeng.* **2002**, *77*, 564−576.

(27) Mattes, T. E.; Coleman, N. V.; Spain, J. C.; Gossett, J. M. Physiological and molecular analyses of vinyl chloride and ethene biodegradation in *Norcardioides* sp. strain JS614. *Arch. Microbiol.* **2005**, *183*, 95−106.

(28) Coleman, N. V.; Spain, J. C. Epoxyalkane:Coenzyme M Transferase in the Ethene and Vinyl Chloride Biodegradation Pathways of *Mycobacterium* Strain JS60. *J. Bacteriol.* **2003**, *185*, 5536−5545.

(29) EPA "Vinyl Fluoride (CAS # 75-02-5)", 1990.

(30) Tu, L. Q.; Chen, y.-Y.; Wright, P. F. A.; Rix, C. J.; Bolton-Grob, R.; Ahokas, J. T. Characterization of the fluoroacetate detoxification enzymes of rat liver cytosol. *Xenobiotica* **2005**, *35*, 989−1002.

(31) Chaojie, Z.; Qi, Z.; Ling, C.; Yuan, Y.; Hui, Y. Degradation of mono-fluorophenols by an acclimated activated sludge. *Biodegradation* **2006**, E-pub ahead of print.

(32) Key, B. D.; Howell, R. D.; Criddle, C. S. Defluorination of organofluorine sulfur compounds by *Pseudomonas* sp. strain D2. *Environ. Sci. Technol.* **1998**, *32*, 2283−2287.

(33) Streger, S. H.; Condee, C. W.; Togna, A. P.; DeFlaun, M. F. Degradation of hydrohalocarbons and brominated compounds by methane- and propane-oxidizing bacteria. *Environ. Sci. Technol.* **1999**, *33*, 4477−4482.